

## Full-length article

# Characteristics of Ca<sup>2+</sup>-exocytosis coupling in isolated mouse pancreatic $\beta$ cells<sup>1</sup>

Qian GE<sup>2,4</sup>, Yong-ming DONG<sup>2,4</sup>, Zhi-tao HU<sup>2</sup>, Zheng-xing WU<sup>2,5</sup>, Tao XU<sup>2,3,5</sup>

<sup>2</sup>College of Life Science and Technology, Huazhong University of Science and Technology, Wuhan 430074, China; <sup>3</sup>National Laboratory of Biomacromolecules, Institute of Biophysics, Chinese Academy of Sciences, Beijing 100101, China

## Key words

mouse; pancreatic  $\beta$  cells; Ca<sup>2+</sup>-exocytosis coupling

<sup>1</sup> Project supported by the National Natural Science Foundation of China (30270363, 30470448 and 30130230), and the National High Technology Research and Development Program of China (2004CB720000). The laboratory of Tao XU is supported by the Partner Group Scheme of the Max Planck Institute for Biophysical Chemistry, Göttingen, and the Sino-German Scientific Center.

<sup>4</sup> These authors contribute equally to this work.

<sup>5</sup> Correspondence to Tao XU.

Phn 86-10-6488-8469.

Fax 86-10-6486-7566.

E-mail xutao@ibp.ac.cn

and Zheng-xing WU.

Phn 86-27-8779-2026, ext 87.

Fax 86-27-8779-2024.

E-mail ibbwuzx@mail.hust.edu.cn

Received 2006-04-16

Accepted 2006-05-21

doi: 10.1111/j.1745-7254.2006.00398.x

## Abstract

**Aim:** To characterize Ca<sup>2+</sup>-stimulated exocytosis in isolated mouse pancreatic  $\beta$  cells. **Methods:** An improved method was described for isolation of mouse pancreatic  $\beta$  cells by collagenase P. The Ca<sup>2+</sup> channel current and the membrane capacitance were examined by using the whole-cell patch clamp recording technique. **Results:** Using depolarization and flash photolysis of caged Ca<sup>2+</sup> to induce Ca<sup>2+</sup>-dependent exocytosis in  $\beta$  cell from KM mouse, we have explored the characteristics of the Ca<sup>2+</sup> channel current and the relationship between Ca<sup>2+</sup> signals and exocytosis. The averaged peak Ca<sup>2+</sup> current measured at +20 mV was  $-60 \pm 6$  pA ( $n=13$ ). **Conclusion:** We characterized three kinetically different pools of vesicles in mouse pancreatic  $\beta$  cells, namely an immediately releasable pool, a readily releasable pool, and a reserve pool.

## Introduction

Glucose homeostasis is critical to the health or survival of mammals and is maintained, in large part, by pancreatic  $\beta$  cells, which secrete insulin in response to an increasing concentration of glucose. Pancreatic  $\beta$  cells sense glucose through their glucose metabolism and the resulting increase in the ATP/ADP ratio closes the ATP-sensitive potassium channels (K<sub>ATP</sub> channels)<sup>[1]</sup>. The closure of K<sub>ATP</sub> channels depolarizes  $\beta$  cells and opens voltage-dependent calcium channels to allow Ca<sup>2+</sup> entry. Ca<sup>2+</sup> acts on the exocytotic machinery to stimulate fusion of insulin-containing vesicles with the plasma membrane for releasing insulin into the bloodstream<sup>[2]</sup>. As Ca<sup>2+</sup> plays a pivotal role in insulin secretion, it

is worthwhile to characterize the Ca<sup>2+</sup> channel activity and the relationship between the Ca<sup>2+</sup> signal and the exocytosis in the pancreatic  $\beta$  cell. In this study, we aimed at establishing an efficient method to isolate healthy pancreatic  $\beta$  cell from the mouse model, and for characterizing the relationship between Ca<sup>2+</sup> signaling and exocytosis in those cells. The reason for choosing the mouse is to open up the possibility for future functional studies of insulin secretion employing the genetic modified mouse model.

## Materials and methods

**Preparation and culture of  $\beta$  cells** Pancreatic  $\beta$  cells from adult male Kunming (KM) mice were prepared as de-

scribed in a previous study<sup>[3,4]</sup> with modifications. In brief, 3–4 week-old KM male mice were killed by cervical dislocation and the pancreas was quickly removed and placed in a 35-mm dish containing cold Hanks' balanced salt solution (HBSS). After being washed for 3 times, the pancreas was minced into tiny tissue blocks and transferred to 50 mL Falcon tube with 40 mL cold HBSS. After removing the supernatant, the tissue blocks were digested by adding 5 mL pre-warmed HBSS containing collagenase P (5 mg/mL, Roche) into the tube and maintained at 37 °C for 40 min in a shaking bath. The digestion was terminated by adding 20 mL cold HBSS solution with 10 % serum, and then centrifuged at 1000 rpm to remove supernatant. The digested tissues were transferred to a dish and the pancreas islets were picked out with a 200  $\mu$ L pipette tip by hand. The isolated islets obtained were dissociated into single cells by vigorous shaking in  $\text{Ca}^{2+}$ - $\text{Mg}^{2+}$ -free HBSS. The dispersed  $\beta$  cells were plated on glass coverslips pre-coated with poly-*L*-lysine and grown in RPMI 1640 medium supplemented with 10 % (*v/v*) fetal bovine serum (FBS), 100  $\mu$ g/mL streptomycin, 100 IU/mL penicillin and 10 mmol/L glucose at 37 °C gassed with a humidified mixture of 5%  $\text{CO}_2$  and 95% air. Cells cultured for 3–5 d were used in the experiments.

**Solutions and drugs** Standard HBSS contained 0.14 g/L  $\text{CaCl}_2$ , 0.1 g/L  $\text{MgCl}_2 \cdot 6\text{H}_2\text{O}$ , 0.1 g/L  $\text{MgSO}_4 \cdot 7\text{H}_2\text{O}$ , 0.4 g/L KCl, 0.06 g/L  $\text{KH}_2\text{PO}_4$ , 0.35 g/L  $\text{NaHCO}_3$ , 8 g/L NaCl, 0.48 g/L  $\text{Na}_2\text{HPO}_4$ , 1 g/L glucose, 20 mmol/L HEPES and 1 mg/mL BSA (pH=7.2; adjusted with NaOH, osmolarity=310 mOsm).

$\text{Ca}^{2+}$ - $\text{Mg}^{2+}$ -free HBSS solution contained 0.4 g/L KCl, 0.06 g/L  $\text{KH}_2\text{PO}_4$ , 0.35 g/L  $\text{NaHCO}_3$ , 8 g/L NaCl, 0.48 g/L  $\text{Na}_2\text{HPO}_4$ , 1 g/L Glucose, addition of 1 mmol/L EGTA, 20 mmol/L HEPES and 10 mg/mL BSA (pH=7.2, 310 mOsm).

RPMI medium 1640 (Gibco) was supplemented with of 10% FBS (Gibco), 100  $\mu$ g/mL streptomycin, 100 IU/mL penicillin and 10 mmol/L glucose.

Standard bath solution for the experiments contained 138 mmol/L NaCl, 5.6 mmol/L KCl, 2.6 mmol/L  $\text{CaCl}_2$ , 1.2 mmol/L  $\text{MgCl}_2$ , 5 mmol/L glucose, and 10 mmol/L HEPES (pH 7.2, 310 mOsm). For depolarization experiments, the bath solution contained 10 mmol/L  $\text{CaCl}_2$  and 20 mmol/L tetraethylammonium-Cl (TEA-Cl). For preparing pipette solutions, we generally prepared 2 $\times$  buffers, which contained 250 mmol/L Cs-glutamate and 80 mmol/L HEPES (pH 7.2). The standard electrode pipette solution contained 125 mmol/L Cs-glutamate, 40 mmol/L HEPES, 2 mmol/L MgATP, 0.3 mmol/L  $\text{Na}_2\text{GTP}$ , 1 mmol/L  $\text{MgCl}_2$  and 0.1 mmol/L EGTA (pH 7.2 adjusted with 1 mol/L CsOH, 300 mOsm). Internal solution for UV-flash photolysis consisted of 110 mmol/L Cs-glutamate, 2 mmol/L MgATP, 0.3 mmol/L  $\text{Na}_2\text{GTP}$ , 35 mmol/L HEPES, 5

mmol/L NP-EGTA [nitrophenyl-ethylene glycol-*bis* ( $\beta$ -aminoethyl ether)-*N,N,N',N'*-tetraacetic acid, NP-FGTA, Molecular Probes, Carlsbad, CA, USA], and 0.2 mmol/L  $\text{Ca}^{2+}$  indicator fura-2 (Molecular Probes), and was adjusted to pH 7.2 with either HCl or CsOH and to osmolarity around 300 mOsm. The free  $\text{Ca}^{2+}$  concentration of the pipette solution was determined to be approximately 200 nmol/L.

**Patch clamp recording and membrane capacitance measurement** Patch clamp electrodes with a resistance of 2–3 M $\Omega$  were made from borosilicate glass capillaries, coated with Sylgard 184 (Dow Corning, Midland, Michigan, USA) and heat-polished. The membrane capacitance ( $C_m$ ) of primary  $\beta$  cell was measured in real time using an EPC9 amplifier (Heka Electronics, Lambrecht, Germany) in conventional whole-cell patch clamp configuration with series resistance ( $R_s$ ) between 5 to 12 M $\Omega$ . A sine+DC protocol was applied using the Lock-In extension of the Pulse program (Heka Electronics). The  $\beta$  cells were voltage clamped at a holding potential of -70 mV and a sine wave voltage command with amplitude of 20 mV and frequency of 977 Hz was applied. Currents were filtered at 2.9 kHz and sampled at 15.6 kHz.

**Flash photolysis** Homogenous global  $[\text{Ca}^{2+}]_i$  elevation was generated by photolysis of the caged- $\text{Ca}^{2+}$  compound, NP-EGTA with UV light generated from a Rapp flash lamp (Rapp Optoelektronik, Hamburg, Germany).  $[\text{Ca}^{2+}]_i$  was measured using dual wavelength excitation method. A series of illuminations alternating between 350 and 380 nm were applied, which allowed ratiometric determination of the  $\text{Ca}^{2+}$  concentration according to the equation:  $[\text{Ca}^{2+}]_i = K_{\text{eff}} \times (R - R_{\text{min}}) / (R_{\text{max}} - R)$ .  $K_{\text{eff}}$ ,  $R_{\text{min}}$ , and  $R_{\text{max}}$  are constants obtained from *in vivo* calibration. The duration of the illuminations was adjusted to maintain relatively constant  $\text{Ca}^{2+}$  concentrations, as the illumination at 350 and 380 nm also lead to photolytic release of  $\text{Ca}^{2+}$ . Trains of light alternating at 350 and 380 nm were generated from a Polychrome IV (Till Photonics, Planegg, Germany). The resulting fluorescence was recorded with a photodiode (Till Photonics).

**Statistical analysis** Data analysis was performed in IGOR Pro 4.02 (WaveMetrics, Lake Oswego, OR, USA), and results were presented as mean $\pm$ SEM with the indicated number of experiments.

## Results

**$\text{Ca}^{2+}$  channel current in KM mouse  $\beta$  cells** We selected cells with diameters 8–10  $\mu$ m for study, so that >80%–90% of the cells were expected to be  $\beta$  cells<sup>[5]</sup>. TEA-containing extracellular solution and intracellular  $\text{Cs}^+$  were used to block most of the voltage-gated  $\text{K}^+$  channels. From recording in

whole-cell configuration with a holding potential of -70 mV,  $\beta$  cells exhibited inward currents typical for  $\text{Ca}^{2+}$  current in response to depolarizing voltage ramped from -70 to +70 mV (Figure 1A). Figure 1B shows slowly inactivating L-type  $\text{Ca}^{2+}$  currents ( $I_{\text{Ca-L}}$ ) evoked by depolarizing step pulses of 100 ms duration from a holding potential of -70 mV to +50 mV in 10 mV increments. The rundown of  $I_{\text{Ca-L}}$  was minimized by intracellular supplement of MgATP (2 mmol/L) and  $\text{Na}_2\text{GTP}$  (0.3 mmol/L). The averaged peak  $\text{Ca}^{2+}$  current measured at +20 mV was  $-60 \pm 6$  pA ( $n=13$ ). The current-voltage relation-

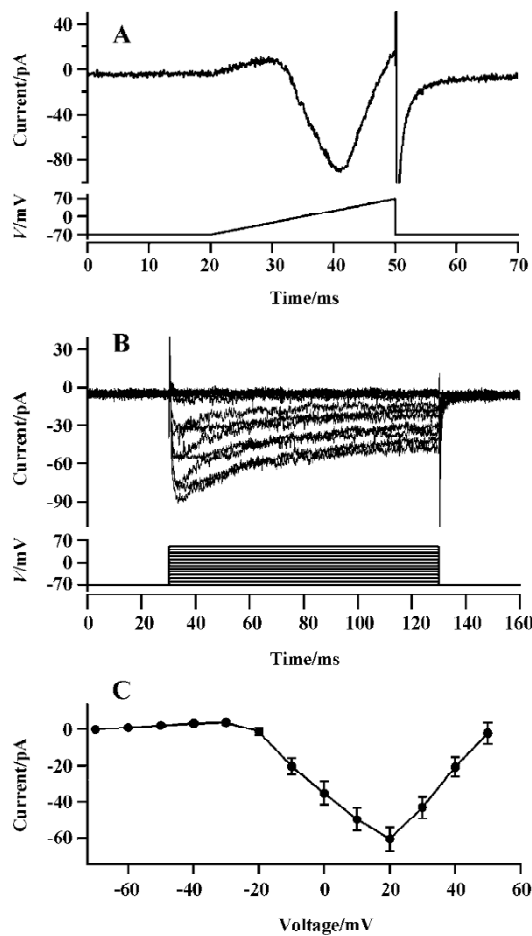


**Figure 1.** KM mouse  $\beta$  cells display activities of L-type  $\text{Ca}^{2+}$  channels. Example trace shows currents (upper panel) evoked by depolarizing voltage ramp from -70 to +70 mV (bottom panel) in a  $\beta$  cell. The  $\text{K}^+$  channel was blocked by  $\text{Cs}^+$  and TEA. Stimulating by step voltage from -70 to +70 mV in 10 mV increments (bottom panel), a slowly inactivating  $\text{Ca}^{2+}$  current in KM mouse  $\beta$  cell was recorded. The experiments were performed by using the standard whole-cell configuration with the  $\text{Cs}^+$ -containing pipette solution and the standard extracellular solution containing 10 mmol/L-extracellular  $\text{Ca}^{2+}$  and 20 mmol/L TEA. Current ( $I$ )-voltage ( $V$ ) relationships of L-type  $\text{Ca}^{2+}$  currents averaged from 13  $\beta$  cells. Mean $\pm$ SEM.

ships ( $I$ - $V$ , shown in Figure 1C) of L-type  $\text{Ca}^{2+}$  were obtained by 100 ms depolarization applied in 10 s-intervals, from holding potential -70 mV to +50mV in 10 mV increments.

**Exocytotic response to pulse depolarization in KM mouse  $\beta$  cells** Exocytosis of a vesicle incorporates its vesicular membrane into the plasma membrane. This leads to an increase in the cell-surface membrane, which can be monitored electrically as an increase in  $C_m$  as it is proportional to the cell-surface membrane.  $C_m$  measurement has the advantage of monitoring secretion from the whole population of vesicles with millisecond time resolution. Pulse voltage, which depolarizes cell membrane and elicits  $\text{Ca}^{2+}$  influx, is recognized as a somewhat physiological stimulus. By using capacitance measurement and simultaneously current recording, the exocytotic response and  $\text{Ca}^{2+}$  current in primary  $\beta$  cells from KM mice were characterized. A typical response was shown in Figure 2A. Pulse voltage stimuli of 90 mV (from the holding potential -70 mV to +20 mV) elicited distinct  $\text{Ca}^{2+}$  current and exocytotic responses. Increasing the duration of the depolarization resulted in more  $\text{Ca}^{2+}$  influx, and larger  $C_m$  increments. For depolarization duration <15 ms, no consistent  $C_m$  increase was detected. The average secretory

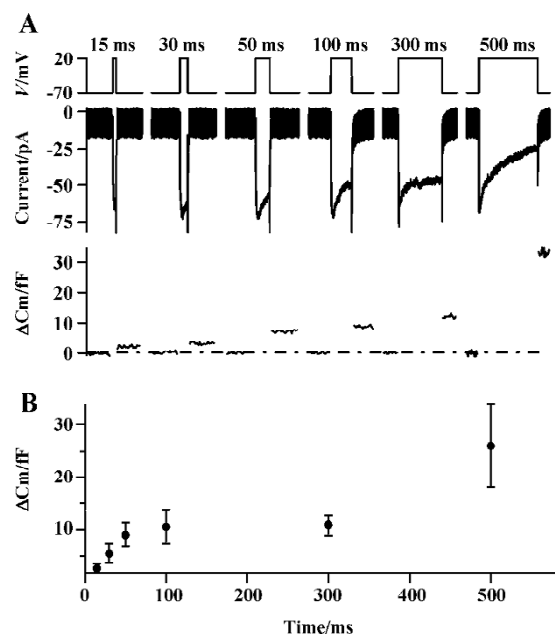


**Figure 2.** Secretion triggered by pulse depolarizations with various duration in  $\beta$  cell. A typical experiment shows  $\text{Ca}^{2+}$  channel current (middle panel) and the increase of membrane capacitance (bottom panel) in primary  $\beta$  cell from KM mouse, stimulated by various pulse depolarizations from -70 to 20 mV with duration ranged from 15 to 500 ms (upper panel). The averaged exocytotic responses ( $n=12$ ) elicited by pulse depolarization shown in (A).

responses from 12 cells are summarized in Figure 2B, in which the average amplitudes of Cm increments were displayed against the duration of the depolarizing pulse. The amplitudes of secretion increased exponentially with a duration shorter than 100 ms, and reached a plateau at durations from 100 to 300 ms. Depolarization pulse of 500 ms in duration elicited further increases in Cm (Figure 2).

**Immediately releasable pool is situated close to the Ca<sup>2+</sup> channel** Ca<sup>2+</sup>-dependent exocytosis can, at least in the short term, be functionally divided into the release of vesicles from a readily releasable pool (RRP) and the subsequent refilling of the RRP from a reserve pool<sup>[6]</sup>. We hypothesized that this also applied to mouse pancreatic  $\beta$  cells and that secretion reflects the sequential release of the two pools of secretory granules. A subset of RRP is spatially arranged in close association to Ca<sup>2+</sup>-channels, thus forming a so-called immediately releasable pool (IRP) that will exocytose instantaneously upon opening of the Ca<sup>2+</sup>-channels.

We explored the relationship between IRP, RRP and Ca<sup>2+</sup> channels by voltage-clamp depolarization shown in Figure 3. The stimulation protocol consisted of a train of five 30-ms depolarizations followed by nine 100-ms pulses from -70 mV to 20 mV. In response to this stimulation protocol, we observed a small Cm increment (16 fF) after the first five pulses representing exocytosis from IRP, and a large exocytosis (254 fF) after the following nine pulses representing exocytosis from RRP.

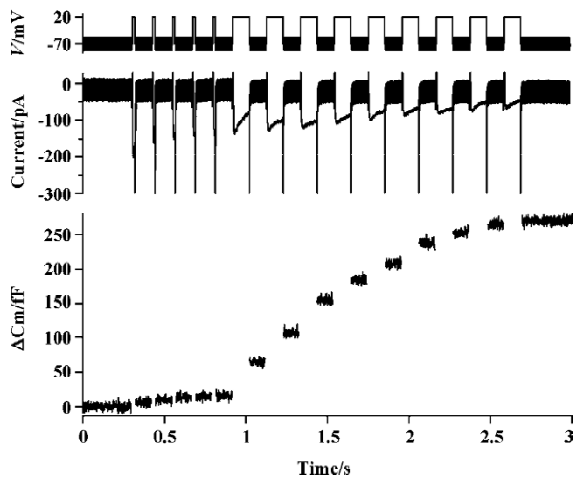


**Figure 3.** Trains of depolarizations elicit distinct exocytosis from IRP and RRP in  $\beta$  cell. Trains of pulse depolarization consisting of five 30-ms and nine 100-ms pulses (upper panel) triggered Ca<sup>2+</sup> currents (middle panel) and exocytotic events (bottom panel) in primary mouse pancreatic  $\beta$  cell. The initial five exocytotic events represent exocytosis from IRP, and the following nine events are secretion from RRP.

**Kinetics of exocytosis and endocytosis in KM mouse  $\beta$  cells** To determine the [Ca<sup>2+</sup>]<sub>i</sub> dependence of vesicles, a well-defined [Ca<sup>2+</sup>]<sub>i</sub> stimulation is necessary. Here we used Ca<sup>2+</sup> uncaging from photolabile caged-Ca<sup>2+</sup> to generate a homogenous [Ca<sup>2+</sup>]<sub>i</sub> elevation, to avoid the complications of Ca<sup>2+</sup> microdomains as a result of local influx, Ca<sup>2+</sup> buffering and mobilization<sup>[7]</sup>. As shown in Figure 4, the Cm increase in response to step-like [Ca<sup>2+</sup>]<sub>i</sub> elevation starts with an exocytotic burst component (within 1 s after flash) followed by a linear sustained release in mouse  $\beta$  cells. It is generally held that the exocytotic burst represents the release from RRP and the sustained phase of secretion is thought to reflect the rate-limiting step of refilling of RRP<sup>[6,8]</sup>. Detailed exami-

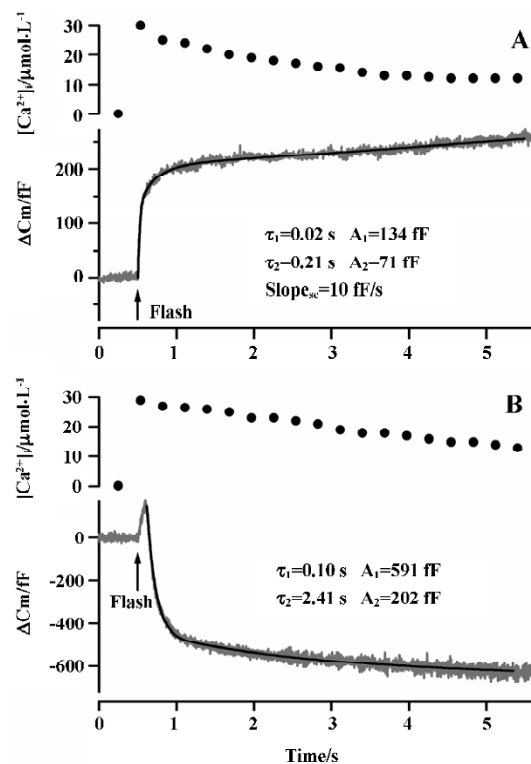


**Figure 4.** Exocytosis and endocytosis in KM mouse pancreatic  $\beta$  cells elicited by step-like [Ca<sup>2+</sup>]<sub>i</sub> elevation by photolysis of caged Ca<sup>2+</sup>. A typical trace of exocytosis in primary  $\beta$  cell from KM mouse triggered by step-like [Ca<sup>2+</sup>]<sub>i</sub> elevation. Kinetic analysis showed the exocytotic trace was best fitted by triple exponential function, shown by the superimposed black curve, indicating the existence of three distinct exocytotic phases. The rate constant ( $\tau$ ) and amplitude (A) of the burst component are:  $\tau_1=20$  ms,  $A_1=134$  fF for the fast burst and  $\tau_2=210$  ms,  $A_2=71$  fF for the slow burst. Example trace of an endocytotic event after flash photolysis. The endocytosis occurred immediately after instantaneous increase of membrane capacitance. The time course of endocytosis exhibited two distinct phases, which was best fitted by double exponential function as shown by the black superimposed curve (B).

nation of the exocytotic burst revealed a double exponential time course, indicating the presence of two releasable vesicle pools with distinct release kinetics<sup>[6]</sup>. The exocytotic burst can be best described by a sum of two exponential components: a fast burst component with a release rate of approximately  $50 \text{ s}^{-1}$ , and a slow burst component with a much slower release rate of approximately  $5 \text{ s}^{-1}$ . The sustained component has a slope of  $10 \text{ fF/s}$ , corresponding to a supplying rate of 3 granules/s if we assume approximately 3 fF for one insulin-containing LDCV<sup>[9,10]</sup>. The characteristics of these exocytotic components were not significantly different from previous studies on mouse  $\beta$  cells<sup>[10,11]</sup>.

Secretion needs a balance between vesicle exocytosis and endocytosis to keep constant cell surface. In  $\beta$  cells, exocytosis is frequently accompanied by endocytosis with a latency of around 300 ms. We measured 22 endocytotic events out of 28 cells. Figure 4B showed a typical trace. The time course of endocytosis was best fitted by a double exponential function, indicating that there existed two endocytotic components. The rate ( $1/\tau$ ) of the fast endocytosis was much faster than that of the slow one, as indicated in Figure 4B. The time constants and amplitudes of both components were:  $\tau_1=0.10 \text{ s}$ ,  $A_1=591 \text{ fF}$  for fast endocytosis; and  $\tau_2=2.41 \text{ s}$ ,  $A_2=202 \text{ fF}$  for slow endocytosis.

## Discussion

We present in this paper an improved method for isolation of  $\beta$  cells from the KM mouse pancreas. Compared with other methods described in previous studies, our method possesses the following advantages: (1) only single enzyme treatment (collagenase P) instead of multiple enzymes is required, therefore, the isolation becomes simple and easy to manipulate; (2)  $\text{Ca}^{2+}$ - $\text{Mg}^{2+}$ -free HBSS was used to dissociate the pancreas islets into a single cell. The relative weak digestion by a single enzyme keeps the membrane protein including receptors and channels less destroyed. Thus, this method could be widely used in  $\beta$  cell isolation.

In mouse pancreatic  $\beta$  cells, insulin is released by  $\text{Ca}^{2+}$ -dependent exocytosis initiated by  $\text{Ca}^{2+}$  entering through voltage-gated L-type  $\text{Ca}^{2+}$  channels<sup>[12]</sup>. And  $\text{Ca}^{2+}$  channels have been shown to co-localize with insulin-containing secretory granules<sup>[13]</sup>. Bokvist *et al* demonstrated that the  $\text{Ca}^{2+}$  transient need extend no more than 1 mm from the plasma membrane to trigger exocytosis<sup>[14]</sup>.

Using trains of short pulse depolarization, an immediately releasable pool (IRP) of vesicles is characterized in the  $\beta$  cell of KM mouse. The IRP is found in numerous endocrine cells. It is generally recognized that the IRP, which is a distinct subset of RRP, is situated in the vicinity of the  $\text{Ca}^{2+}$

channel<sup>[15]</sup>. Thus, vesicles sensor a relative higher  $\text{Ca}^{2+}$  level and release faster in response to trains of depolarization.

$\text{Ca}^{2+}$  is a triggering signal for neurotransmitter and hormone release.  $\text{Ca}^{2+}$  diffusion yields an immediate accumulation of calcium ions within an area covering tens of nanometers around the mouth of open  $\text{Ca}^{2+}$  channels. This calcium signal can be restrained by the buffering action of  $\text{Ca}^{2+}$ -binding proteins. Local  $\text{Ca}^{2+}$  influx and buffering will result in qualitatively different types of intracellular signals, depending on the spatial arrangement of  $\text{Ca}^{2+}$  channels relative to each other and to the relevant  $\text{Ca}^{2+}$ -binding proteins. The variety of  $\text{Ca}^{2+}$  signals that vesicles sense complicate the analysis of  $\text{Ca}^{2+}$  dependence and kinetics of vesicle release. By employing photolysis of caged  $\text{Ca}^{2+}$  to generate a spatial homogenous  $[\text{Ca}^{2+}]_i$  elevation as stimuli for secretion, we characterized the kinetics of exocytosis and endocytosis in the primary  $\beta$  cell of KM mouse. Flash experiments reveal that the exocytotic response to step-like  $\text{Ca}^{2+}$  elevation exhibits three kinetic components, in consistence with previous studies in pancreatic beta cells<sup>[10,11]</sup>.

Endocytosis is an important cellular function, by which the increased plasma membrane is taken up into cell, and the released vesicles are renewed and reused. Fast and slow modes of endocytosis are found at a number of synapses and in various cells. Our high-time resolution capacitance measurement demonstrated the existence of two endocytotic components in  $\beta$  cells of KM mouse. Until now, the molecular mechanism underlying the fast endocytosis still remains elusive<sup>[16]</sup>. The fast endocytosis is characterized by a very fast endocytotic rate ( $1/\tau > 1 \text{ s}^{-1}$ ) and amplitude normally exceeding that of exocytosis<sup>[17,18]</sup>. The underlying mechanism is still unknown. Further analysis of the  $\text{Ca}^{2+}$ -dependent exocytosis and endocytosis in pancreatic  $\beta$  cells from genetic manipulated mouse model will be necessary for elucidating the underlying mechanism.

## References

- 1 Eliasson L, Renstrom E, Ding WG, Proks P, Rorsman P. Rapid ATP-dependent priming of secretory granules precedes  $\text{Ca}^{2+}$ -induced exocytosis in mouse pancreatic  $\beta$ -cells. *J Physiol* 1997; 503: 399–412.
- 2 MacDonald PE, Rorsman P. Oscillations, intercellular coupling, and insulin secretion in pancreatic beta cells. *PLoS Biol* 2006; 4: 49.
- 3 Wan QF, Dong Y, Yang H, Lou X, Ding J, Xu T. Protein kinase activation increases insulin secretion by sensitizing the secretory machinery to  $\text{Ca}^{2+}$ . *J Gen Physiol* 2004; 124: 653–62.
- 4 Chen L, Koh DS, Hille B. Dynamics of calcium clearance in mouse pancreatic beta-cells. *Diabetes* 2003; 52: 1723–31.
- 5 Rorsman P, Trube G. Calcium and delayed potassium currents in mouse pancreatic beta-cells under voltage-clamp conditions. *J*

- Physiol 1986; 374: 531–50.
- 6 Sorensen JB. Formation, stabilisation and fusion of the readily releasable pool of secretory vesicles. *Pflugers Arch* 2004; 448: 347–62.
  - 7 Neher E. Vesicle pools and Ca<sup>2+</sup> microdomains: new tools for understanding their roles in neurotransmitter release. *Neuron* 1998; 20: 389–99.
  - 8 Xu T, Binz T, Niemann H, Neher E. Multiple kinetic components of exocytosis distinguished by neurotoxin sensitivity. *Nat Neurosci* 1998; 1:192–200.
  - 9 Gopel S, Zhang Q, Eliasson L, Ma XS, Galvanovskis J, Rorsman P, *et al*. Capacitance measurements of exocytosis in mouse pancreatic alpha-, beta- and delta-cells within intact islets of Langerhans. *J Physiol* 2004; 556: 711–26.
  - 10 Olofsson CS, Gopel SO, Barg S, Galvanovskis J, Rorsman P, Eliasson L, *et al*. Fast insulin secretion reflects exocytosis of docked granules in mouse pancreatic  $\beta$ -cells. *Pflugers Arch* 2002; 444: 43–51.
  - 11 Takahashi N, Kadowaki T, Yazaki Y, Miyashita Y, Kasai H. Multiple exocytotic pathways in pancreatic  $\beta$  cells. *J Cell Biol* 1997; 138: 55–64.
  - 12 Ammala C, Eliasson L, Bokvist K, Larsson O, Ashcroft FM, Rorsman P. Exocytosis elicited by action potentials and voltage-clamp calcium currents in individual mouse pancreatic  $\beta$ -cells. *J Physiol* 1993; 472: 665–88.
  - 13 Wisler O, Trus M, Hernandez A, Renstrom E, Barg S, Rorsman P, *et al*. The voltage sensitive Lc-type Ca<sup>2+</sup> channel is functionally coupled to the exocytotic machinery. *Proc Natl Acad Sci USA* 1999; 96: 245–53.
  - 14 Bokvist K, Eliasson L, Ammala C, Renstrom E, Rorsman P. Colocalization of L-type Ca<sup>2+</sup> channels and insulin-containing secretory granules and its significance for the initiation of exocytosis in mouse pancreatic  $\beta$ -cells. *EMBO J* 1995; 14: 50–7.
  - 15 Ammala C, Eliasson L, Bokvist K, Larsson O, Ashcroft FM, Rorsman P. Exocytosis elicited by action potentials and voltage-clamp calcium currents in individual mouse pancreatic  $\beta$ -cells. *J Physiol* 1993; 472: 665–88.
  - 16 Harata NC, Choi S, Pyle JL, Aravanis AM, Tsien RW. Frequency-dependent kinetics and prevalence of kiss-and-run and reuse at hippocampal synapses studied with novel quenching methods. *Neuron* 2006; 49: 243–56.
  - 17 Heinemann C, Chow RH, Neher E, Zucker RS. Kinetics of the secretory response in bovine chromaffin cells following flash photolysis of caged Ca<sup>2+</sup>. *Biophys J* 1994; 67: 2546–57.
  - 18 Smith C, Neher E. Multiple forms of endocytosis in bovine adrenal chromaffin cells. *J Cell Biol* 1997; 139: 885–94.